

Observation of plasmon-phonons in a metamaterial superconductor using inelastic neutron scattering

Vera N. Smolyaninova¹⁾, Jeffrey W. Lynn²⁾, Nicholas P. Butch²⁾, Heather Chen-Mayer²⁾, Joseph C. Prestigiacomo³⁾, M. S. Osofsky³⁾, and Igor I. Smolyaninov^{4,5)}

¹⁾*Department of Physics Astronomy and Geosciences, Towson University,*

8000 York Rd., Towson, MD 21252, USA

²⁾*NIST Center for Neutron Research, National Institute of Standards and Technology,*

100 Bureau Drive, Gaithersburg, MD 20899-6102, USA

³⁾*Naval Research Laboratory, Washington, DC 20375, USA*

⁴⁾*Department of Electrical and Computer Engineering, University of Maryland, College Park, MD 20742, USA*

⁵⁾*Saltenna LLC, 1751 Pinnacle Drive #600 McLean, VA 22102, USA*

Metamaterial approach is capable of drastically increasing the critical temperature, T_c , of composite metal-dielectric superconductors. Tripling of T_c was observed in bulk Al-Al₂O₃ core-shell metamaterials. A theoretical model based on the Maxwell-Garnett approximation provides a microscopic explanation of this effect in terms of electron-electron pairing mediated by a hybrid plasmon-phonon excitation. We report the first observation of this excitation in Al-Al₂O₃ core-shell metamaterials using inelastic neutron scattering. This result provides support for this novel mechanism of superconductivity in metamaterials and explains the 50 year old mystery of enhanced T_c in granular aluminium films.

Recent theoretical [1-3] and experimental [4-6] work has demonstrated that many tools developed in electromagnetic metamaterial research can be successfully used to engineer artificial metamaterial superconductors having considerably improved superconducting properties. This connection between electromagnetic metamaterials and superconductivity research stems from the fact that superconducting properties of a material may be expressed via its effective dielectric response function $\epsilon_{\text{eff}}(q, \omega)$, where Kirzhnits, Maksimov and Khomskii [7] demonstrated that the critical temperature, T_c , of a conventional superconductor is defined by the behaviour of its inverse dielectric response function $\epsilon^{-1}(q, \omega)$ near its poles. In conventional superconductors these poles are defined by the dispersion law, $\omega(q)$, of phonons which mediate electron-electron pairing. Recently, we have demonstrated a considerable enhancement of the attractive electron-electron interaction in such metamaterial scenarios as epsilon near zero (ENZ) composite superconductor-dielectric [8] and hyperbolic metamaterials [9] since, in both cases, the inverse dielectric response function of the metamaterial may exhibit additional poles compared to the parent superconductor. The most striking example of successful metamaterial superconductor engineering was the recent observation of tripling of the critical temperature T_c in Al-Al₂O₃ epsilon near zero (ENZ) core-shell metamaterials compared to bulk aluminium [5]. The formation of these bulk Al-Al₂O₃ samples enable studies that require large sample volumes, such as neutron diffraction, that can reveal phonon spectral features that are not accessible in thin films.

Here, we report on the use of inelastic neutron scattering to provide the first experimental evidence of an excitation that does not exist in pure Al and corresponds to the metamaterial pole of the engineered inverse dielectric response function responsible for the T_c enhancement in this material. We also identify the microscopic physical origin of this additional metamaterial pole as coming from a hybrid plasmon-phonon mode which arises in a composite metal-dielectric metamaterial. The hybrid character of this mode enables efficient inelastic neutron scattering from its phonon component,

which is observed in the experiment. The direct observation of plasmon-phonon modes in Al-Al₂O₃ ENZ core-shell metamaterials using inelastic neutron scattering provides strong support of this novel plasmon-phonon mechanism of superconductivity in composite metal-dielectric ENZ metamaterials.

The theoretical model of superconductivity in ENZ metamaterials is based on the paper by Kirzhnits *et al.* [7], which demonstrated that within the framework of macroscopic electrodynamics the electron-electron interaction in a superconductor may be expressed in the form of an effective Coulomb potential

$$V(\vec{q}, \omega) = \frac{4\pi e^2}{q^2 \varepsilon_{\text{eff}}(\vec{q}, \omega)} = \frac{V_C}{\varepsilon_{\text{eff}}(\vec{q}, \omega)}, \quad (1)$$

where $V_C = 4\pi e^2/q^2$ is the Fourier-transformed Coulomb potential in vacuum, and $\varepsilon_{\text{eff}}(q, \omega)$ is the linear dielectric response function of the superconductor treated as an effective medium. The critical temperature of a superconductor in the weak coupling limit is typically calculated as

$$T_c = \theta \exp\left(-\frac{1}{\lambda_{\text{eff}}}\right), \quad (2)$$

where θ is the characteristic temperature for a bosonic mode mediating electron pairing (such as the Debye temperature θ_D in the standard BCS theory) [10]. The dimensionless coupling constant λ_{eff} is defined by $V(q, \omega) = V_C \varepsilon^{-1}(q, \omega)$ and the density of states ν (see for example [11]):

$$\lambda_{\text{eff}} = -\frac{2}{\pi} \nu \int_0^{\infty} \frac{d\omega}{\omega} \langle V_C \text{Im} \varepsilon^{-1}(\vec{q}, \omega) \rangle, \quad (3)$$

where V_C is the unscreened Coulomb repulsion, and the angle brackets denote average over the Fermi surface. Now this formalism will be applied to a composite metal-dielectric metamaterial.

Following [12], a simplified dielectric response function of a metal may be written as

$$\varepsilon_m(q, \omega) = \left(1 + \frac{k^2}{q^2}\right) \left(1 - \frac{\Omega^2(q)}{\omega^2 + i\omega\Gamma}\right) \quad (4)$$

where k is the inverse Thomas-Fermi screening radius, $\Omega(q)$ is the dispersion law of a phonon mode, and Γ is the corresponding damping rate. The zero of the dielectric response function of the bulk metal (which occurs at $\omega = \Omega(q)$ where ε_m changes sign) maximizes the electron-electron pairing interaction given by Eq. (1). This simplified consideration of $\varepsilon_m(q, \omega)$ has been justified in [3].

A superconducting metallic “matrix” with dielectric “inclusions”, which forms a composite metal-dielectric metamaterial, is now considered. We will assume that the permittivity ε_d of the dielectric does not depend on (q, ω) and stays positive and constant. According to the Maxwell-Garnett effective medium approximation [13], mixing of nanoparticles of a superconducting “matrix” with dielectric “inclusions” (described by the dielectric constants ε_m and ε_d , respectively) results in an effective medium with a dielectric constant ε_{eff} , which may be obtained as

$$\left(\frac{\varepsilon_{\text{eff}} - \varepsilon_m}{\varepsilon_{\text{eff}} + 2\varepsilon_m}\right) = (1-n) \left(\frac{\varepsilon_d - \varepsilon_m}{\varepsilon_d + 2\varepsilon_m}\right), \quad (5)$$

where n is the volume fraction of metal ($0 \leq n \leq 1$). The explicit expression for $\varepsilon_{\text{eff}}^{-1}$ may be written as

$$\varepsilon_{\text{eff}}^{-1} = \frac{n}{(3-2n)} \frac{1}{\varepsilon_m} + \frac{9(1-n)}{2n(3-2n)} \frac{1}{(\varepsilon_m + (3-2n)\varepsilon_d/2n)} \quad (6)$$

For a given value of the metal volume fraction n , the ENZ conditions ($\varepsilon_{eff} \approx 0$) may be obtained around $\varepsilon_m \approx 0$ (at the phonon frequency $\omega = \Omega(q)$ of the superconducting metal), and around

$$\varepsilon_m \approx -\frac{3-2n}{2n} \varepsilon_d \quad . \quad (7)$$

According to Eq. (4), the additional pole of the inverse dielectric response function described by Eq. (7) occurs at some frequency $\omega < \Omega(q)$ close to the phonon resonance. Indeed, Eqs. (4) and (7) allow us to predict the location of the additional pole with respect to the phonon frequency $\Omega(q)$, based on the magnitude of the dielectric permittivity ε_d of the insulator used in the metamaterial design. Neglecting the unknown value of Γ in Eq.(4), we obtain:

$$\varepsilon_m(q, \omega) \approx \left(1 + \frac{k^2}{q^2}\right) \left(1 - \frac{\Omega^2(q)}{\omega^2}\right) \approx -\frac{3-2n}{2n} \varepsilon_d \quad . \quad (8)$$

This leads to the following expression for the ratio of the additional pole and the regular phonon frequencies:

$$\frac{\omega}{\Omega} \approx \left(1 + \frac{(3-2n)\varepsilon_d}{2n\left(1 + \frac{k^2}{q^2}\right)}\right)^{-1/2} \quad . \quad (9)$$

The dielectric constant for aluminium oxide in the long wavelength infrared (LWIR) range is $\varepsilon_d \sim 2.25$. Using the ratio of the inverse Thomas-Fermi radius to the Fermi radius for aluminium $k/k_F = 1.17$ tabulated in [12], and assuming $q=2k_F$, the ω/Ω ratio given by Eq. (9) may be calculated as a function of n . This function is shown in Fig. 1. Based on these estimates, we may expect that the additional pole must be located in the $0.4\Omega - 0.7\Omega$ range depending on the volume fraction of aluminum in the metamaterial.

To search for the existence of this additional excitation, which should occur at frequencies lower than the phonon frequencies of aluminium, an inelastic neutron scattering experiment was performed. To prepare the samples, commercial (US Research Nanomaterials, Inc.) 18 nm diameter aluminium nanoparticles were oxidized under ambient conditions. Upon oxidation, an approximately 2 nm thick layer of Al_2O_3 is formed on the surface of aluminium nanoparticles [14]. The particles were subsequently compressed into dense pellets in a hydraulic press. An SEM image of such a core-shell Al- Al_2O_3 compressed sample is shown in Fig. 2(a). It was taken using LoVac APREO Scanning Electron Microscope. The superconducting transition of this bulk metamaterial sample was measured to be $T_c = 3.7$ K, which is more than three times higher than $T_c = 1.2$ K of bulk aluminium (Fig. 2 (b)). The zero-field cooled magnetization data shown in Fig. 2(b) were measured using MPMS SQUID magnetometer in magnetic field of 10 G (10 G = 1 mT). The T_c enhancement in this sample is similar to that reported in our previous work [5].

The inelastic neutron scattering experiments were performed at the NIST Center for Neutron Research using triple-axis spectrometers BT7 [15] and BT4 and the Disk Chopper Spectrometer. For the measurements on BT-7 we employed horizontal focusing with a fixed final energy $E_f = 14.7$ meV to increase the range of the wave vector integration. A pyrolytic graphite filter was used in the scattered beam and a velocity selector in the incident beam to suppress higher-order wavelength contaminations and reduce background [15]. Data were collected in the energy range from 3 to 43 meV at 5 K employing a closed cycle helium refrigerator. The high energy data were collected on BT-4 Filter Analyzer Neutron Spectrometer using the Cu(220) monochromator. Data were obtained from 36 meV to 250 meV in a 78 K in a liquid

nitrogen cryostat. Background data were obtained with the sample lifted out of the beam area. The highest resolution data were collected on the Disk Chopper Spectrometer [16] in a pumped ^4He cryostat. Data were collected at 1.5 K and 6 K, below and above the superconducting transition temperature of 3.7 K respectively, with an incident energy of 13 meV. In subtracting the 6 K data from the 1.5 K data, we found a small but noticeable increase in the scattering in the superconducting state over a broad energy range from just above the elastic line to ≈ 8 meV. This behaviour is typical for inelastic scattering experiments with superconductors.

The results from inelastic neutron scattering measurements at $T = 5$ K are shown in Fig. 3. The sample was thermally treated at 110°C in vacuum before the measurements to remove possible water adsorbed on the particles. Data above 40 meV are dominated by scattering from hydrogen in the form of OH [17], which may come from a small amount of AlOOH. Prompt gamma-ray neutron activation analysis [18,19] showed a hydrogen content of 12 atomic percent H in the sample. The neutron scattering cross section for H is 80.27 compared to Al of 1.5, which is why the H can contribute to the scattering at high energies even though the amount of H is relatively small.

Fig. 3 (b) shows data for energies below 43 meV, taken at wave vectors $Q = 4 \text{ \AA}^{-1}$, 4.25 \AA^{-1} , and 4.5 \AA^{-1} , which are proportional to the generalized phonon density of states (PDOS), which is the phonon density-of-states weighted by the neutron cross sections. The PDOS for bulk aluminum at $T = 10$ K (black circles) [20] is shown for comparison. Two peaks in the aluminium PDOS corresponding to transverse and longitudinal acoustical phonons are also present in core-shell Al-Al₂O₃ metamaterial, which are indicated with black arrows in Fig. 3 (b). However, there is an additional peak at around 15 meV (indicated with blue arrow), which is not present in pure aluminum. This peak cannot be attributed to the aluminum oxide, since aluminum

oxide has a stiffer lattice [21], and will have a peak in the PDOS at energies higher than that for aluminium. Therefore, we have observed an additional contribution to the PDOS which was predicted by our metamaterial model at energies within the span of phonon energies of aluminium. This peak is also consistent with unexplained extra spectral weight seen at low energy in the $\alpha^2F(\omega)$ extracted from the tunnelling conductance of granular Al films that is absent in pure Al films [22]. Since this quantity is a direct measure of the boson mechanism responsible for superconductivity, it is reasonable to infer that the observed peak reflects a contribution to mechanism responsible for the enhanced T_c in our metamaterial samples. We should also recall that in 1968, Cohen and Abeles observed that the superconductive transition temperature, T_c , of thin films of granular aluminium (Al grains coated with Al_2O_3) was significantly higher than that of bulk Al ($\sim 1.2\text{K}$) [23]. Several mechanisms were proposed to explain this enhancement but none has proven to be satisfactory. Our observations provide an explanation for this 50 year old mystery of enhanced T_c in granular aluminium thin films.

Now we discuss the microscopic physical origin of these additional excitations. According to Eq. (7), at $n = 0.75$ the resonant conditions occur at $\epsilon_m = -\epsilon_d$, which corresponds to the dispersion law of surface plasmons propagating along planar metal-dielectric interfaces [24]:

$$k = \frac{\omega}{c} \left(\frac{\epsilon_m \epsilon_d}{\epsilon_m + \epsilon_d} \right)^{1/2} . \quad (10)$$

For non-planar interfaces of aluminium nanoparticles the plasmon resonance occurs at slightly different points (depending on the interface curvature). However, Eqs. (7) and (10) clearly relate the additional pole of the inverse dielectric response function $\epsilon_{\text{eff}}^{-1}$ of the metamaterial to the plasmon resonance at metal-dielectric interfaces. On the other hand, since this additional plasmon resonance of the metamaterial structure may exist only in the vicinity of the metal phonon at $\omega = \Omega(q)$ (where ϵ_m changes sign), the proper

name of this resonant excitation should probably be chosen as a “hybrid” plasmon-phonon resonance. Unlike regular plasmons in metals (which typically occur in the visible and infrared frequency ranges) the hybrid plasmon-phonon mode in metal-dielectric composite metamaterials occurs near the frequency range of conventional phonons. This means that hybrid plasmon-phonons are coupled to lattice vibrations via the lattice polarizability, which enables their detection via inelastic neutron scattering.

Based on Eqs. (2, 3), it is clear that the existence of an additional plasmon-phonon pole of the inverse dielectric response function $\epsilon_{\text{eff}}^{-1}$ of the metamaterial may lead to increased T_c . The microscopic physical origin of this effect may be illustrated by Fig. 4(a). As pointed out in [25], plasmon-mediated pairing of electrons may be understood in terms of image charge-mediated Coulomb interaction. Let us consider two electrons located next to a planar interface between two media with dielectric permittivities ϵ_1 and ϵ_2 , as shown in Fig. 4(a). The field acting on the charge e_2 in the medium ϵ_1 at $z > 0$ is obtained as a superposition of fields produced by the charge e_1 and its image e_1' [26]. As a result, the effective Coulomb potential may be obtained as

$$V = \frac{e}{\epsilon_1} \left(\frac{e}{r_1} - \frac{e}{r_2} \left(\frac{\epsilon_2 - \epsilon_1}{\epsilon_2 + \epsilon_1} \right) \right), \quad (11)$$

which may be simplified as

$$V = \frac{2e^2}{r(\epsilon_2 + \epsilon_1)} \quad (12)$$

if both charges are located very close to the interface, so that $r_1 = r_2 = r$. As mentioned above, the $\epsilon_2 = -\epsilon_1$ condition, which maximizes the electron pairing interaction, corresponds to the dispersion law of surface plasmons propagating along the interface (see Eq. (10)).

The values of λ_{eff} due to each pole in Eq. (6) may be evaluated in terms of λ_m for the bulk metal, assuming that ν in Eq.(3) is proportional to n , which is justified by the

fact that there are no free charges in the dielectric phase of the metamaterial. We assume that $\text{Im}(\varepsilon_d) \sim 0$ and neglect the dispersion of $\text{Im}(\varepsilon_m)$ in this simplified estimate (the detailed calculations may be found in [3]). Near the plasmon-phonon pole

$$\text{Im}(\varepsilon_{eff}^{-1}) \approx \frac{9(1-n)}{2n(3-2n)\varepsilon_m''} \quad (13)$$

where $\varepsilon_m'' = \text{Im}(\varepsilon_m)$. Therefore, using Eq. (3), we may obtain the expression for λ_{eff} as a function of λ_m and n for the plasmon-phonon pole:

$$\lambda_{eff} \approx \frac{9(1-n)}{2(3-2n)} \lambda_m, \quad (14)$$

where λ_m for the parent superconductor is determined by Eq.(3) in the $n \rightarrow 1$ limit. On the other hand, near the regular phonon pole the inverse dielectric response function of the metamaterial behaves as

$$\text{Im}(\varepsilon_{eff}^{-1}) \approx \frac{n}{(3-2n)\varepsilon_m''} \quad (15)$$

Therefore, near this pole

$$\lambda_{eff} \approx \frac{n^2}{(3-2n)} \lambda_m \quad (16)$$

Assuming the known values $T_{cbulk} = 1.2$ K and $\theta_D = 428$ K of bulk aluminium [27], Eq. (2) results in $\lambda_m = 0.17$, which corresponds to the weak coupling limit. In order to make the mechanism behind the enhancement of T_c in the Al-Al₂O₃ core-shell metamaterial superconductor abundantly clear, let us plot the hypothetic values of T_c as a function of metal volume fraction n , which would originate from either Eq. (14) or Eq. (16) in the absence of each other. The corresponding values calculated as

$$T_c = T_{Cbulk} \exp\left(\frac{1}{\lambda_m} - \frac{1}{\lambda_{eff}}\right) \quad (17)$$

which are shown in Fig. 4b. The vertical dashed line corresponds to the assumed critical value of the metal volume fraction n_{cr} at which the additional plasmon-phonon pole of ϵ_{eff}^{-1} disappears as $n \rightarrow 0$ (since according to Eq. (4) the magnitude of ϵ_m is limited). The blue dashed line shows the predicted behaviour in the presence of both poles [3]. The experimentally measured data points from [5] are shown for comparison on the same plot. The match between the experimentally measured values of enhanced T_c and the theoretical curve obtained based on Eq. (17) is quite impressive, given the fact that our model does not contain any free parameters. Such a good match, along with the previously mentioned measurements of $\alpha^2 F(\omega)$, implies that the plasmon-phonon mediated electron pairing is the physical mechanism responsible for the tripling of T_c in the Al-Al₂O₃ core-shell metamaterial superconductor.

In conclusion, we have observed a low energy excitation in Al-Al₂O₃ composite ENZ core-shell metamaterials using inelastic neutron scattering that doesn't exist in pure Al. A scenario based on plasmons at the Al-Al₂O₃ interface interacting with Al phonons can account for the observations. This result provides strong support for the novel plasmon-phonon mechanism of superconductivity in ENZ metamaterials and accounts for the enhanced T_c observed in granular aluminum thin films.

We thank Terrance J. Udovic for helpful discussions about hydrogen phonon modes and W. Zimmerman and B. Augstein for experimental help. This work was supported in part by the DARPA Award No: W911NF-17-1-0348 "Metamaterial Superconductors," NSF MRI Award No: 1626326, the Office of Naval Research (ONR) through the Naval Research Laboratory Basic Research Program, and Towson University School of Emerging Technologies grant. The identification of any

commercial product or trade name does not imply endorsement or recommendation by the National Institute of Standards and Technology.

References

- [1] I. I. Smolyaninov, V. N. Smolyaninova, Is there a metamaterial route to high temperature superconductivity?, *Adv. Cond. Matt. Phys.* **2014**, 479635 (2014).
- [2] I. I. Smolyaninov, V. N. Smolyaninova, Metamaterial superconductors, *Phys. Rev. B* **91**, 094501 (2015).
- [3] I. I. Smolyaninov, V. N. Smolyaninova, Theoretical modelling of critical temperature increase in metamaterial superconductors, *Phys. Rev. B* **93**, 184510 (2016).
- [4] V. N. Smolyaninova, B. Yost, K. Zander, M. S. Osofsky, H. Kim, S. Saha, R. L. Greene, I. I. Smolyaninov, Experimental demonstration of superconducting critical temperature increase in electromagnetic metamaterials, *Scientific Reports* **4**, 7321 (2014).
- [5] V. N. Smolyaninova, K. Zander, T. Gresock, C. Jensen, J. C. Prestigiacomo, M. S. Osofsky, I. I. Smolyaninov, Using metamaterial nanoengineering to triple the superconducting critical temperature of bulk aluminum, *Scientific Reports* **5**, 15777 (2015).
- [6] V. N. Smolyaninova, C. Jensen, W. Zimmerman, J.C. Prestigiacomo, M. S. Osofsky, H. Kim, N. Bassim, Z. Xing, M. M. Qazilbash, I. I. Smolyaninov, Enhanced superconductivity in aluminum-based hyperbolic metamaterials, *Scientific Reports* **6**, 34140 (2016).

- [7] D. A. Kirzhnits, E. G. Maksimov, D. I. Khomskii, The description of superconductivity in terms of dielectric response function, *J. Low Temp. Phys.* **10**, 79 (1973).
- [8] N. Engheta, Pursuing near-zero response, *Science* **340**, 286 (2013).
- [9] Z. Jakob, L. V. Alekseyev, E. Narimanov, Optical hyperlens: far-field imaging beyond the diffraction limit, *Optics Express* **14**, 8247 (2006).
- [10] V. L. Ginzburg, Nobel Lecture: On superconductivity and superfluidity, *Rev. Mod. Phys.* **76**, 981-998 (2004).
- [11] E. A. Pashitskii, Plasmon mechanism of high temperature superconductivity in cuprate metal-oxide compounds, *JETP* **76**, 425-444 (1993).
- [12] N. W. Ashcroft, N. D. Mermin, *Solid State Physics* (Saunders, New York, 1976) pp. 515-518.
- [13] T. C. Choy, *Effective Medium Theory* (Clarendon Press, Oxford, 1999).
- [14] T.-S. Shih, Z.-B. Liu, Thermally-formed oxide on aluminum and magnesium, *Materials Transactions* **47**, 1347 (2006).
- [15] J. W. Lynn, Y. Chen, S. Chang, Y. Zhao, S. Chi, W. Ratcliff, II, B. G. Ueland, R. W. Erwin, Double Focusing Thermal Triple Axis Spectrometer at the NCNR, *Journal of Research of NIST* **117**, 61-79 (2012).
- [16] J. R. D. Copley, J. C. Cook, The Disk Chopper Spectrometer at NIST: a new instrument for quasielastic neutron scattering studies, *Chemical Physics* **292**, 477 – 485 (2003).

- [17] G. Paglia, C. E. Buckley, T. J. Udovic, A. L. Rohl, F. Jones, C. F. Maitland, J. Connolly, Boehmite-Derived γ -Alumina System. 2. Consideration of Hydrogen and Surface Effects, *Chem. Mater.* **16**, 1914-1923 (2004).
- [18] R.L. Paul, D. Şahin, J.C. Cook, *et al.*, NGD cold-neutron prompt gamma-ray activation analysis spectrometer at NIST, *J Radioanal Nucl Chem* **304**, 189–193 (2015);
- [19] D. Turkoglu, H. Chen-Mayer, R. Paul, R. Zeisler, Assessment of PGAA capability for low-level measurements of H in Ti alloys, *Analyst* **142**, 3822–3829 (2017).
- [20] M. Kresch, M. Lucas, O. Delaire, J. Y. Y. Lin, B. Fultz, Phonons in aluminum at high temperatures studied by inelastic neutron scattering, *Phys. Rev. B* **77**, 024301 (2008).
- [21] C. Loyola, E. Menéndez-Proupin, G. Gutiérrez, Atomistic study of vibrational properties of γ -Al₂O₃, *J. Mater. Sci.* **45**, 5094 (2010).
- [22] M. Dayan, Tunneling measurements on crystalline and granular aluminum. *J. of Low Temp Phys.* **32**, 643-655 (1978).
- [23] R. W. Cohen, B. Abeles, Superconductivity in granular aluminum films, *Phys. Rev.* **168**, 444-450 (1968).
- [24] A. V. Zayats, I. I. Smolyaninov, A. Maradudin, Nano-optics of surface plasmon-polaritons, *Physics Reports* **408**, 131-314 (2005).
- [25] M. Rona, Image-charge-mediated pairing in oxide superconductors, *Phys. Rev. B* **42**, 4183-4188 (1990).
- [26] J. D. Jackson, *Classical Electrodynamics* (Wiley, New York, 1998).
- [27] C. Kittel, *Introduction to Solid State Physics* (Wiley, New York, 2004) pp. 260-262, 405.

Figure Captions

Figure 1. Ratio of the plasmon-phonon and the phonon frequencies calculated as a function of metal volume fraction n in the Al-Al₂O₃ metamaterial using Eq.(9). The arrow indicates the frequency of an additional peak observed in the neutron scattering experiment.

Figure 2. (a) Scanning Electron Microscope image of the Al-Al₂O₃ metamaterial. (b) Temperature dependence of zero field cooled magnetization per unit mass for fresh and oxidized Al-Al₂O₃ core-shell metamaterial samples made of 18 nm aluminium nanoparticles. The observed onset of superconductivity at ~ 3.7 K in the oxidized sample is 3.25 times larger than $T_c = 1.2$ K of bulk aluminium [5]. The inset shows photo of the compressed metamaterial sample (note: $1 \text{ emu} = 10^{-3} \text{ A m}^2$).

Figure 3. (a) Inelastic neutron scattering data obtained for the core-shell Al-Al₂O₃ metamaterial at energies below 250 meV. The lower-energy data were obtained on BT-7 and the high energy data were taken on BT-4 FANS. Data above 40 meV are dominated by scattering from hydrogen in the form of OH, which may come from a small amount of AlOOH in the metamaterial. (b) Inelastic neutron scattering data for energies below 43 meV taken on BT-7, averaged over measurements taken at wave vectors $Q = 4 \text{ \AA}$, 4.25 \AA , and 4.5 \AA . Uncertainties originate from counting statistics and correspond to one standard deviation. The averaged dependence is proportional to the generalized phonon density of states (PDOS). The DOS for bulk aluminum at $T = 10$ K (black circles) [20] is shown for comparison. Two peaks which are indicated with black arrows in the aluminium PDOS correspond to the van-Hove peaks for the transverse and longitudinal acoustical phonons, respectively, at the Brillouin zone boundaries. They are also present in the core-shell Al-Al₂O₃ metamaterial. The additional peak at around 15 meV (indicated with blue arrow) is not present in pure aluminum. It corresponds to the hybrid plasmon-phonons of the metamaterial.

Figure 4. (a) Schematic view of the surface plasmon resonance geometry: an electron e_2 located next to the interface between two media with dielectric permittivities ϵ_1 and ϵ_2 , interacts with electron e_1 and its image e_1' . Resonant conditions are obtained at $\epsilon_1 = -\epsilon_2$. (b) Plots of the theoretically calculated values of T_c as a function of metal volume fraction n , which would originate from either phonon (Eq. (16), black line) or plasmon-phonon (Eq. (14), red line) pole of the inverse dielectric response function of the Al- Al_2O_3 core-shell metamaterial in the absence of each other. Blue dashed line shows the predicted behaviour in the presence of both poles. The experimentally measured data points from [5] are shown for comparison on the same plot. The vertical dashed line corresponds to the assumed value of n_{cr} .

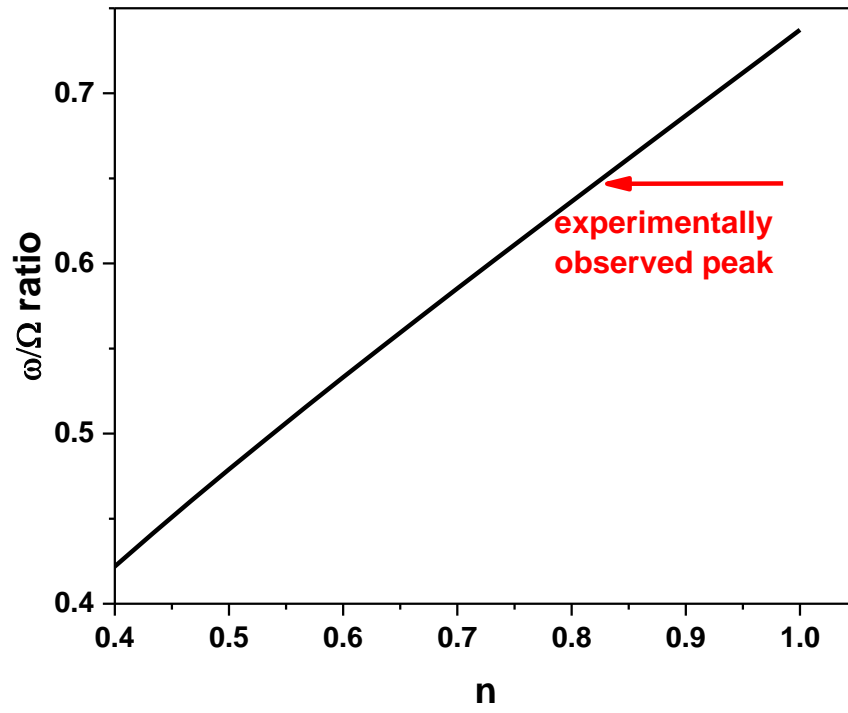


Fig. 1

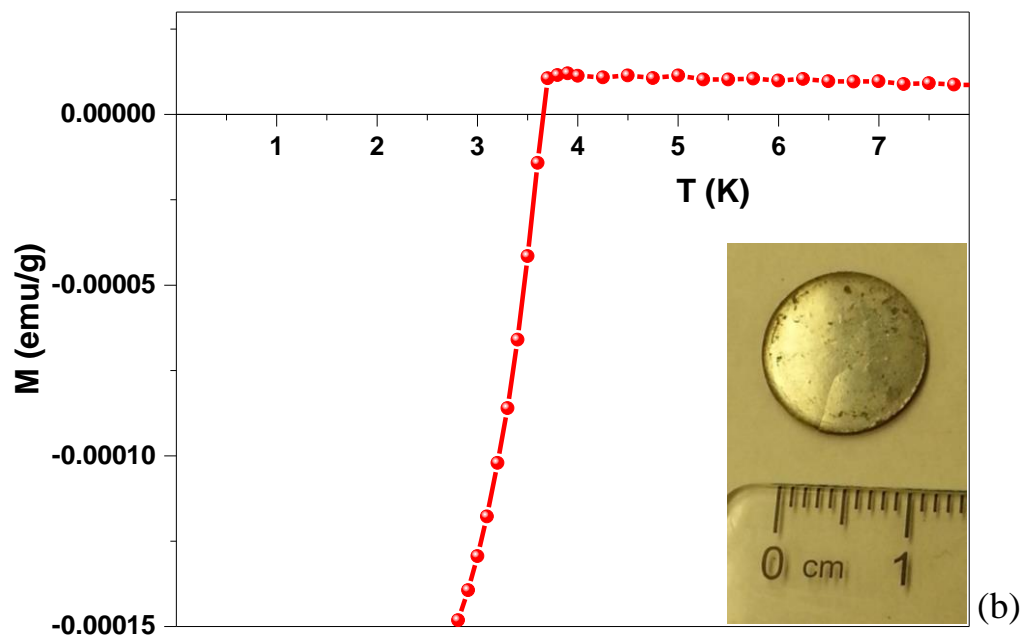
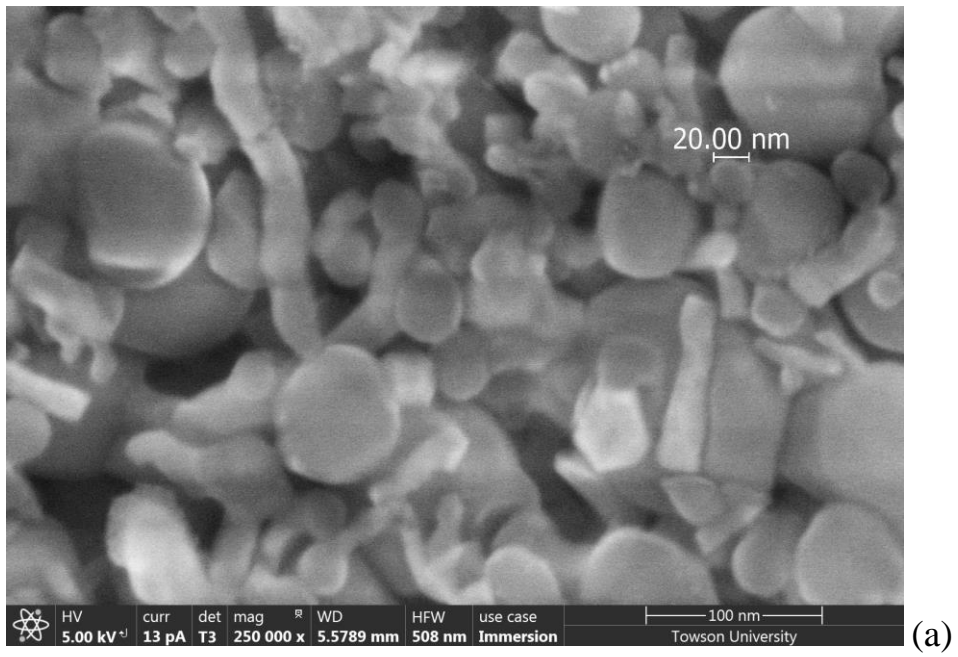
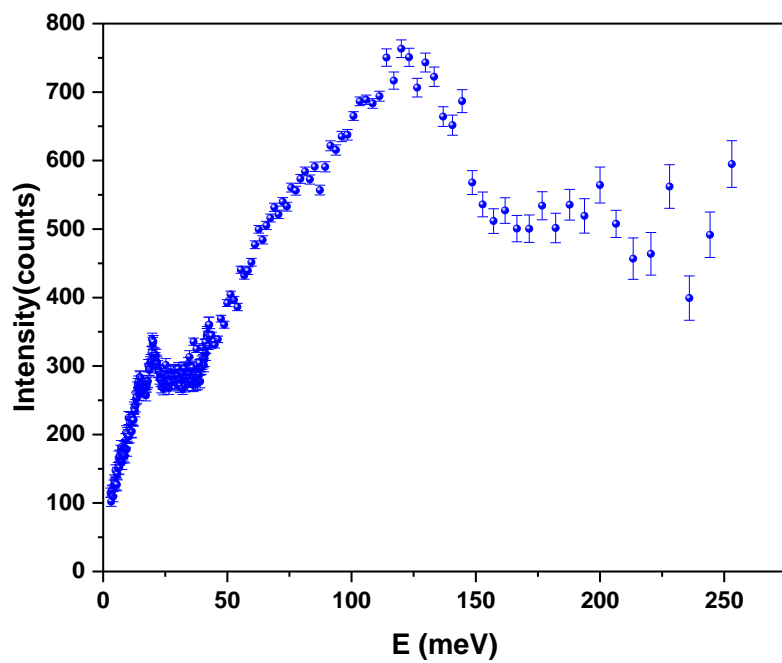
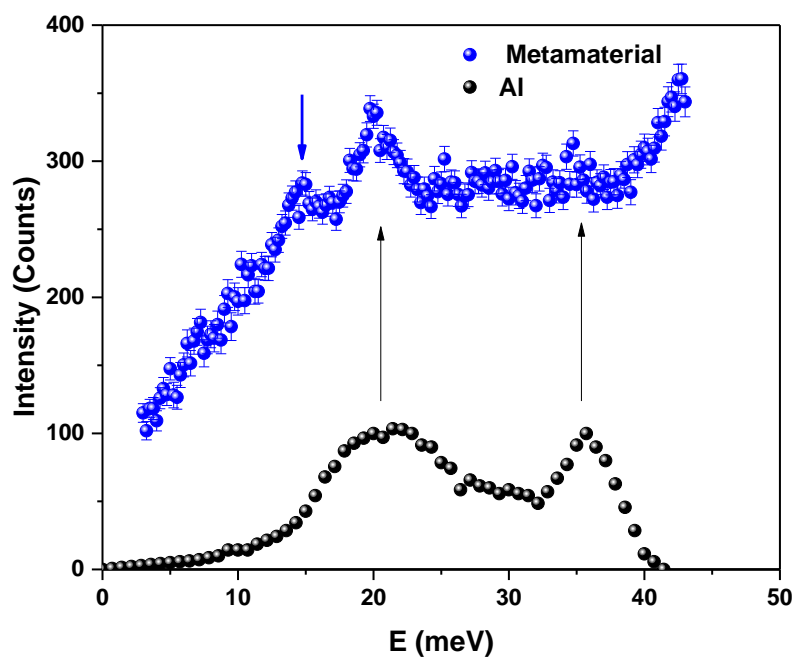


Fig. 2



(a)



(b)

Fig. 3.

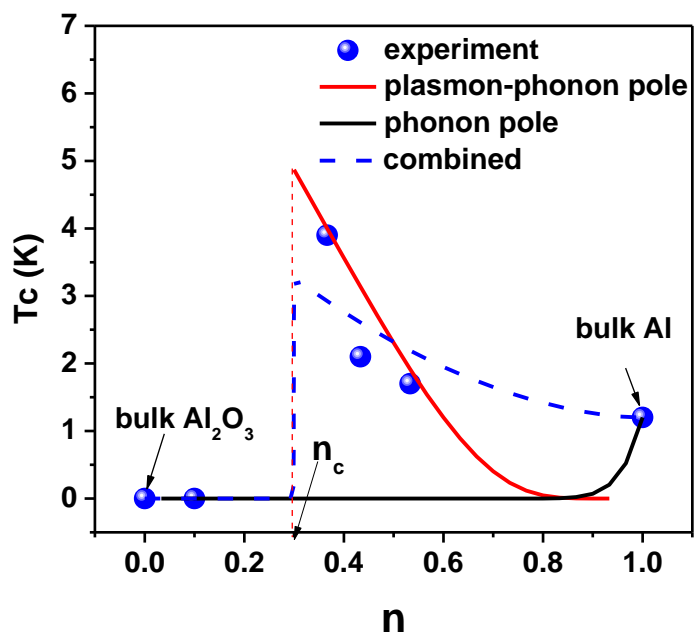
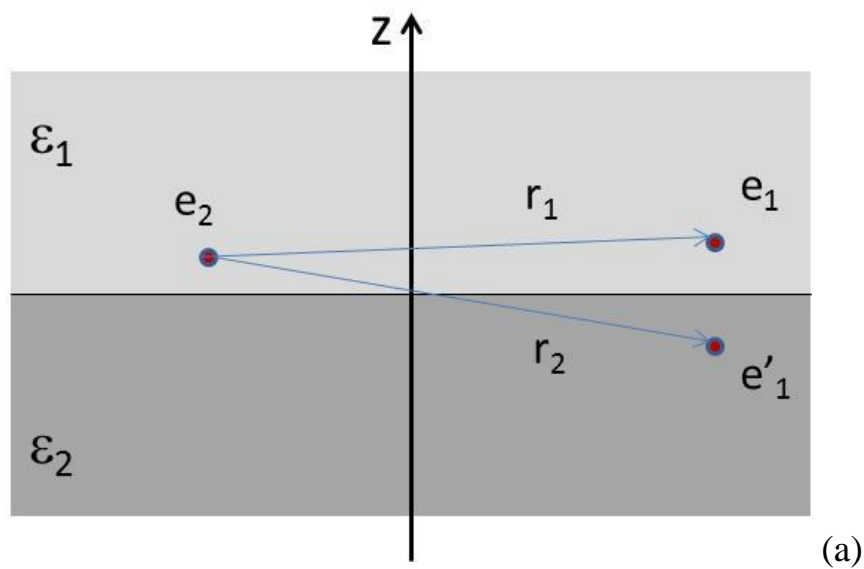


Fig. 4

(b)